Available online at www.sciencedirect.com
SCIENCE DIRECT®
Journal of Sound and Vibration 266 (2003) 1079–1098
JOURNAL OF SOUND AND VIBRATION
www.elsevier.com/locate/jsvi

Application of vortex sound theory to vortex-pairing noise: sensitivity to errors in flow data

C. Schram[a,*], A. Hirschberg[b]

[a] *Von Karman Institute for Fluid Dynamics, Chaussée de Waterloo 72, 1640 Rhode-St-Genèse, Belgium*
[b] *Technische Universiteit Eindhoven, 5600 MB Eindhoven, Netherlands*

Received 3 December 2001; accepted 1 October 2002

Abstract

Aeroacoustical analogies allow one to extract acoustical information from limited information about the flow. In the particular case of low Mach number compact flows, vortex sound theory has been quite successful. In the present paper, different formulations of the vortex sound theory are compared on the basis of their ability to provide realistic results for vortex-pairing sound when approximate flow models are used. In particular, these theories do not perform equally well when applied to a flow model in which the effective conservation of momentum and kinetic energy is not respected, as it should be in the absence of external forces and neglecting viscous dissipation and compressibility effects. A conservative form of the vortex sound theory is obtained by reiterating the assumptions of conservation of these flow invariants. This alternative form of the analogy allows one to obtain more robust results when applied to perturbed analytical flow models and experimental data.

1. Lighthill's analogy

In a recent paper, Fedorchenko [1] states that the acoustical analogy is not a useful concept. In the present paper, it is argued that the acoustical analogy can be quite useful. The use of the subtle approach of Möhring [2] to vortex sound theory is considered. In the original paper and the more extended description provided by Dowling et al. [3], some of the steps in the derivation of this analogy are made quite implicitly. An attempt is made to provide the reader with a more explicit description. The key idea that is stressed is that the analogy allows one to predict sound

*Corresponding author. Tel.: +32-2-359-9611; fax: +32-2-359-9600.
E-mail address: schram@vki.ac.be (C. Schram).

0022-460X/03/$ - see front matter
doi:10.1016/S0022-460X(02)01630-9

production by a flow from experimental data or simplified theoretical models while this would be impossible by a more direct approach.

The main idea of Lighthill's analogy [4] is to deduce an exact equation in which aerodynamic sound sources are made "explicit". By combination of the exact mass and momentum conservation laws, Lighthill obtains

$$\frac{1}{c_0^2}\frac{\partial^2 p}{\partial t^2}-\frac{\partial^2 p}{\partial x_i^2}=\frac{\partial^2(\rho v_i v_j-\sigma_{ij})}{\partial x_i \partial x_j}-\frac{\partial f_i}{\partial x_i}+\frac{1}{c_0^2}\frac{\partial^2 p}{\partial t^2}-\frac{\partial^2 \rho}{\partial t^2}\equiv q, \tag{1}$$

where ρ is the fluid density, v_i are the velocity components, p is the pressure, σ_{ij} is the viscous stress tensor, f_i is an external force density and c_0 is a velocity. The right hand of Eq. (1) defines the acoustical source term q. A set of 4 exact equations (11 unknowns) has been replaced by a single equation (still 11 unknowns). At first glance this seems quite useless. The key to the use of an analogy is to introduce approximations. As stated by Tam [5] this makes the use of the analogy an intuitive procedure with a non-unique solution.

The first approximation is to assume that the listener is submerged into a uniform stagnant fluid with pressure p_0 and density ρ_0. It is assumed that around this listener the flow can be approximated by neglecting all the right side source terms ($q=0$). This defines the wave propagation region, as opposed to the acoustical source region in which $q\neq 0$. The speed of sound c_0 is identified as the speed of sound in the uniform and stagnant fluid surrounding the listener.

A further approximation is to assume that the acoustical source region is limited in space. One would like now to obtain information about the right-hand side q from an analytical theory, numerical simulation or experimental data. An important step is to make this approximation within an integral formulation of the analogy. This integral formulation smoothes out random errors in the flow description [6].

A commonly used and convenient assumption is that the feedback of the acoustic field (outside the source region) on the flow in the source region is negligible. The discussion will be limited to free field conditions for which the acoustical feedback is indeed quite small at low Mach numbers. At low Mach numbers one can also neglect the effect of density fluctuations in the source term.

Additional assumptions such as the absence of external force fields ($f_i=0$) and neglecting the visco-thermal effects [7,8] yield the wave equation:

$$\frac{1}{c_0^2}\frac{\partial^2 p'}{\partial t^2}-\frac{\partial^2 p'}{\partial x_i^2}=\frac{\partial^2 \rho_0 v_i v_j}{\partial x_i \partial x_j}, \tag{2}$$

where p is the acoustical pressure perturbation.

A drawback of Lighthill's analogy is that the source region ($q\neq 0$) can be rather extended in space. Realizing that sound production in an inviscid homentropic flow is determined by the dynamics of vorticity, Powell [9] obtained an alternative to Lighthill's formulation in which the role of vorticity becomes explicit.

This formulation is not only useful because the region in which there is vorticity ($\boldsymbol{\omega}\neq 0$) is often much smaller than the region in which Lighthill's source term is non-vanishing ($q\neq 0$), but also because inviscid homentropic flows at low Mach numbers are most efficiently described in terms of vortex dynamics. When the flow is locally two dimensional, attractive point vortex (or vortex blob) methods can be used. In some cases these point vortex models are very crude and do not even respect momentum nor energy conservation.

The aim of this paper is to show how different versions of the analogy behave when such approximate flow models are used. The example of a free flow: the leapfrogging of two vortex rings is considered, in which the dominating source term should be a quadrupole. The implications of this analysis for experimental work on jet noise is then discussed. The sensitivity of the sound predictions to random perturbations introduced in a simple vortex pairing flow model [10] are investigated. A related discussion of the theory of Howe [11] is provided in another paper [12].

2. Powell's analogy

For low Mach numbers and compact source regions, with no external force field and neglecting visco-thermal effects, the vortex sound analogy is written [9]:

$$\frac{1}{c_0^2}\frac{\partial^2 p'}{\partial t^2}-\frac{\partial^2 p'}{\partial x_i^2}=\frac{\partial}{\partial x_i}\rho_0(\boldsymbol{\omega}\times\mathbf{v})_i+\frac{\partial^2}{\partial x_i^2}\left(\rho_0\frac{|\mathbf{v}|^2}{2}\right), \tag{3}$$

where $\boldsymbol{\omega}$ and $\mathbf{v}$ are respectively the vorticity and velocity.

In absence of solid boundaries, using the free space Green's function

$$G(t,\mathbf{x}|\tau,\mathbf{y})=\frac{\boldsymbol{\delta}(t-\tau-|\mathbf{x}-\mathbf{y}|/c_0)}{4\pi|\mathbf{x}-\mathbf{y}|}, \tag{4}$$

where $\mathbf{x}$ is the listener's position and $\mathbf{y}$ the co-ordinate in the source region, one obtains the integral formulation [3]:

$$p'(\mathbf{x},t)=\frac{\rho_0}{4\pi}\frac{\partial}{\partial x_i}\int_V\left.\frac{(\boldsymbol{\omega}\times\mathbf{v})_i}{|\mathbf{x}-\mathbf{y}|}\right|_{t^*}\mathrm{d}^3\mathbf{y}+\frac{\rho_0}{4\pi}\frac{\partial^2}{\partial x_i^2}\int_V\left.\frac{|\mathbf{v}|^2/2}{|\mathbf{x}-\mathbf{y}|}\right|_{t^*}\mathrm{d}^3\mathbf{y}, \tag{5}$$

where $t^*\equiv t-|\mathbf{x}-\mathbf{y}|/c_0$ is the retarded time. For a compact source region, one can use a Taylor expansion of the retarded time:

$$t^*=t-\frac{|\mathbf{x}|}{c_0}+\frac{\mathbf{x}\cdot\mathbf{y}}{|\mathbf{x}|c_0}+\cdots. \tag{6}$$

Using a far field approximation [3] one finds for the first integral of Eq. (5):

$$\begin{aligned}\frac{\rho_0}{4\pi}\frac{\partial}{\partial x_i}\int_V\left.\frac{(\boldsymbol{\omega}\times\mathbf{v})_i}{|\mathbf{x}-\mathbf{y}|}\right|_{t^*}\mathrm{d}^3\mathbf{y}\simeq&-\frac{\rho_0}{4\pi c_0}\frac{x_i}{|\mathbf{x}|^2}\frac{\partial}{\partial t}\int_V(\boldsymbol{\omega}\times\mathbf{v})_i|_{t_0^*}\,\mathrm{d}^3\mathbf{y}\\&-\frac{\rho_0}{4\pi c_0^2}\frac{x_ix_j}{|\mathbf{x}|^3}\frac{\partial^2}{\partial t^2}\int_V y_j(\boldsymbol{\omega}\times\mathbf{v})_i|_{t_0^*}\,\mathrm{d}^3\mathbf{y},\end{aligned} \tag{7}$$

where the integrands on the right side must be evaluated at the retarded time $t_0^*\equiv t-|\mathbf{x}|/c_0$. It can be shown [13–15] that, owing to the conservation of the impulse

$$P=\frac{1}{2}\rho_0\int_V\mathbf{y}\times\boldsymbol{\omega}\,\mathrm{d}^3\mathbf{y}, \tag{8}$$

that applies in absence of external forces, the first term in Eq. (7) vanishes. The same algebra applied to the second integral in Eq. (5) gives

$$\frac{\rho_0}{4\pi}\frac{\partial^2}{\partial x_i^2}\int_V \frac{|\mathbf{v}|^2/2}{|\mathbf{x}-\mathbf{y}|}\bigg|_{t^*} \mathrm{d}^3\mathbf{y} \simeq \frac{\rho_0}{4\pi c_0}\frac{1}{|\mathbf{x}|}\frac{\partial^2}{\partial t^2}\int_V \frac{|\mathbf{v}|^2}{2}\bigg|_{t_0^*} \mathrm{d}^3\mathbf{y} + \frac{\rho_0}{4\pi c_0^2}\frac{x_j}{|\mathbf{x}|^2}\frac{\partial^3}{\partial t^3}\int_V y_j\frac{|\mathbf{v}|^2}{2}\bigg|_{t_0^*} \mathrm{d}^3\mathbf{y} \tag{9}$$

in which the first term on the left side vanishes, because of the conservation of the kinetic energy

$$T = \rho_0 \int_V \mathbf{y}\cdot(\boldsymbol{\omega}\times\mathbf{v})\,\mathrm{d}^3\mathbf{y}, \tag{10}$$

in an inviscid incompressible flow approximation [13–15]. Moreover, it can be shown [3] that the second term scales with $\rho_0 M^5 l/|\mathbf{x}|$ (where l is a typical eddy size and M is the flow Mach number) and can be neglected at low Mach numbers. This yields the integral solution of Powell's analogy:

$$p'_P(\mathbf{x},t) = -\frac{\rho_0}{4\pi c_0^2|\mathbf{x}|^3}\frac{\partial^2}{\partial t^2}\int_V (\mathbf{x}\cdot\mathbf{y})\,\mathbf{x}\cdot(\boldsymbol{\omega}\times\mathbf{v})|_{t_0^*}\,\mathrm{d}^3\mathbf{y}. \tag{11}$$

Please note that the first integrals in Eqs. (7) and (9) have simply been set equal to zero because one knows that there are no external forces and that kinetic energy is conserved in an inviscid incompressible flow. This occurs even if the calculation of the flow field does not respect these conservation laws.

3. Möhring's analogy

Möhring [2] derived an alternative formulation of Powell's analogy, in which the sound production depends on the evolution of the vorticity alone. Möhring argued that the explicit presence of the flow velocity in Powell's formulation (11) might cause some difficulties when dealing with vortex filaments or vortex sheets, on which the self-induced velocity is singular.

Möhring's analogy is based on the Helmholtz's equation for inviscid and incompressible flow [13,14]:

$$\frac{\partial\boldsymbol{\omega}}{\partial t} + \boldsymbol{\nabla}\times(\boldsymbol{\omega}\times\mathbf{v}) = 0, \tag{12}$$

and on the vectorial identity:

$$\boldsymbol{\nabla}\times[\tfrac{1}{5}(\mathbf{x}\cdot\mathbf{y})\,\mathbf{x}\times\mathbf{y}] = (\mathbf{x}\cdot\mathbf{y})\mathbf{x} - \tfrac{1}{3}|\mathbf{x}|^2\mathbf{y}. \tag{13}$$

Substituting $(\mathbf{x}\cdot\mathbf{y})\mathbf{x}$ from Eq. (13) into Powell's analogy (11), one finds

$$p'(\mathbf{x},t) = -\frac{\rho_0}{12\pi c_0^2|\mathbf{x}|^3}\frac{\partial^2}{\partial t^2}\bigg\{\int_V \boldsymbol{\nabla}\times[(\mathbf{x}\cdot\mathbf{y})\mathbf{x}\times\mathbf{y}]\cdot(\boldsymbol{\omega}\times\mathbf{v})|_{t_0^*}\,\mathrm{d}^3\mathbf{y} + |\mathbf{x}|^2\int_V \mathbf{y}\cdot(\boldsymbol{\omega}\times\mathbf{v})|_{t_0^*}\,\mathrm{d}^3\mathbf{y}\bigg\}. \tag{14}$$

The second integral is proportional to the kinetic energy of flow (10) so that its contribution to the sound pressure vanishes. After integration by parts, and using the Helmholtz equation (12), the

first integral of Eq. (14) becomes

$$\int_V \nabla \times [(\mathbf{x}\cdot\mathbf{y})\mathbf{x}\times\mathbf{y}]\cdot(\boldsymbol{\omega}\times\mathbf{v})\,\mathrm{d}^3\mathbf{y} = -\frac{\partial}{\partial t}\int_V (\mathbf{x}\cdot\mathbf{y})\,\mathbf{x}\cdot(\mathbf{y}\times\boldsymbol{\omega})\,\mathrm{d}^3\mathbf{y} \tag{15}$$

and finally the Möhring's analogy is obtained:

$$p'_M(\mathbf{x},t) = \frac{\rho_0}{12\pi c_0^2|\mathbf{x}|^3}\frac{\partial^3}{\partial t^3}\int_V (\mathbf{x}\cdot\mathbf{y})\mathbf{x}\cdot(\mathbf{y}\times\boldsymbol{\omega})|_{t_0^*}\,\mathrm{d}^3\mathbf{y}. \tag{16}$$

Please note that Möhring's analogy is obtained from Powell's one, with the assumptions already included in that formulation (conservation of momentum and kinetic energy), and by imposing once more the conservation of kinetic energy in absence of viscous dissipation for an incompressible flow. The same conclusion has been reached by Powell [16] who proved the equivalence of the two analogies as a consequence of the conservation of kinetic energy, without invoking any acoustical argument. It is interesting to note that other approaches lead to the formulation of Möhring (16) like the "contiguous method" [17], or methods based on the matched asymptotic expansions [10,18]. A drawback of Möhring's analogy is that its source term is not locally defined (i.e., its value is not invariant under a change of the origin of co-ordinates), while Powell's source $\rho_0\,(\boldsymbol{\omega}\times\mathbf{v})$ is locally defined, which makes its physical interpretation much easier in terms of local sound production. Furthermore, Möhring's approach involves one more time derivative than Powell's formulation, which might induce a stronger sensitivity to errors in the flow model.

4. Special case: sound field of a system of vortex rings

Möhring [2] considered the situation where the vorticity is concentrated into circular vortex ring filaments. Using the same formalism, his approach is generalized to the case of a continuous distribution of vorticity. This allows the application of the analogy to the data obtained from particle image velocimetry measurements (Section 5.3). A flow which has a cylindrical symmetry is considered. The co-ordinate of an element of vorticity is given by

$$\mathbf{y} = z\,\mathbf{n} + r\,\mathbf{e}(\phi), \tag{17}$$

where $\mathbf{n}$ and $\mathbf{e}(\phi)$ are unit vectors, respectively, parallel with and perpendicular to the axis of symmetry (Fig. 1), and z and r are respectively the axial and radial coordinates. The vorticity and velocity are expressed by

$$\begin{aligned}\boldsymbol{\omega}(r,\theta,z) &= \omega(r,z)\,\mathbf{n}\times\mathbf{e}(\phi),\\ \mathbf{v}(r,\theta,z) &= u(r,z)\;\mathbf{n} + v(r,z)\;\mathbf{e}(\phi) + w(r,z)\;\mathbf{n}\times\mathbf{e}(\phi),\end{aligned} \tag{18}$$

where $\boldsymbol{\omega}$ is the azimuthal component of the vorticity $\boldsymbol{\omega}$ and u, v and w are respectively the axial, radial and azimuthal components of the velocity $\mathbf{v}$.

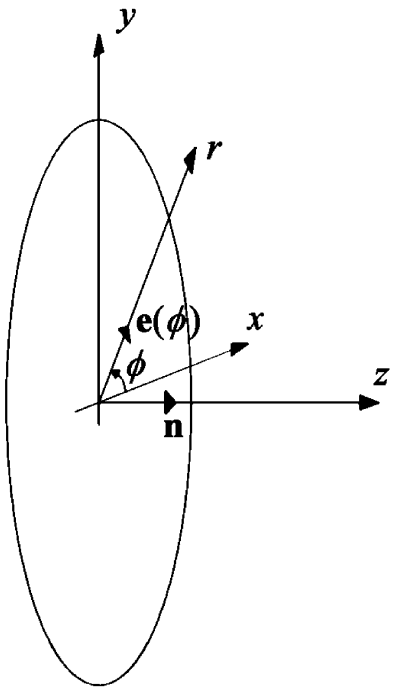

Fig. 1. Circular element of vorticity and co-ordinate system.

Substituting description (18) of the flow into Powell's expression (11) yields

$$p'_P(\mathbf{x},t)=\frac{\rho_0}{4c_0^2|\mathbf{x}|^3}\frac{\partial^2}{\partial t^2}\left\{\left[2\int\int_S \omega vrz\,\mathrm{d}r\,\mathrm{d}z+\int\int_V \omega ur^2\,\mathrm{d}r\,\mathrm{d}z\right]\mathbf{x}\cdot(\mathbf{n}\,\mathbf{n})\cdot\mathbf{x}\right.$$
$$\left.-\int\int_S \omega ur^2\,\mathrm{d}r\,\mathrm{d}z\,(\mathbf{x}\cdot\mathbf{x})\right\} \tag{19}$$

(the specification of the retarded time t_0^* is further left out). The same substitution into Möhring's expression (16) gives

$$p'_M(\mathbf{x},t)=\frac{\rho_0}{4c_0^2|\mathbf{x}|^3}\frac{\mathrm{d}^3Q}{\mathrm{d}t^3}\mathbf{x}\cdot\left(\mathbf{n}\,\mathbf{n}-\frac{\mathbf{I}}{3}\right)\cdot\mathbf{x}, \tag{20}$$

where Q is defined by

$$Q=\int\int_S \omega r^2 z\,\mathrm{d}r\,\mathrm{d}z. \tag{21}$$

5. Application to the leapfrogging of two vortex rings

Different levels of approximation are used below for the description of the pairing of two vortex rings: firstly the periodic leapfrogging of thin core rings is considered (Sections 5.1 and 5.2);

secondly, the application to an experimental description of the flow obtained by particle image velocimetry will be briefly discussed in Section 5.3.

5.1. Two-dimensional modelling

The first model assumes that the initial axial separation between the leading and the trailing ring $d \equiv Z_L - Z_T$ (see Fig. 2) is very small with respect to their initial radius R_0, so that their mutual induction is locally two dimensional. Moreover, the radius of the core σ is assumed to be small compared to d, so that the mutual induction of two vortex filaments is considered. The corresponding evolution law is [2]

$$Z_L(t) = u_0 t + \frac{d}{2}\cos\left(\frac{\Gamma t}{\pi d^2}\right), \quad R_L(t) = R_0 + \frac{d}{2}\sin\left(\frac{\Gamma t}{\pi d^2}\right),$$
$$Z_T(t) = u_0 t - \frac{d}{2}\cos\left(\frac{\Gamma t}{\pi d^2}\right), \quad R_T(t) = R_0 - \frac{d}{2}\sin\left(\frac{\Gamma t}{\pi d^2}\right), \tag{22}$$

where u_0 is the self-induced axial velocity of each vortex ring (assumed constant).

This very simple model neglects the vortex stretching that occurs during slip-through, and whose primary effect is to modulate the self-induced velocity of each ring. The self-induced velocity of a circular vortex ring of radius R, core radius σ and evenly distributed vorticity over its core is [13–15]:

$$U = \frac{\Gamma}{4\pi R}\left(\log\frac{8R}{\sigma} - \frac{1}{4}\right), \tag{23}$$

where Γ is the circulation of the vortex.

The effect of stretching is not important for small initial separation d/R_0 between the vortex rings. This is apparent in Fig. 3 which shows that the trajectory of the cores is similar for $d/R_0 = 0.1$ using the two-dimensional model (22) and the three-dimensional model (40) that will

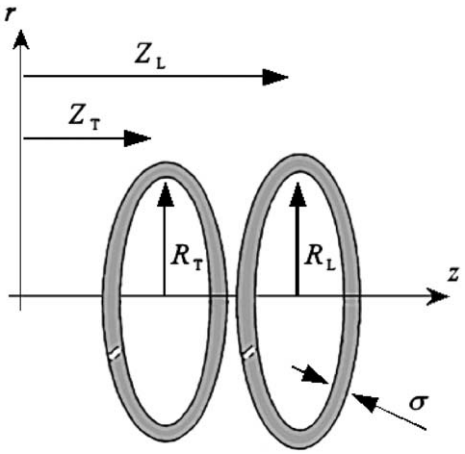

Fig. 2. Initial positions of the leading ring (Z_L, R_L) and of the trailing ring (Z_T, R_T).

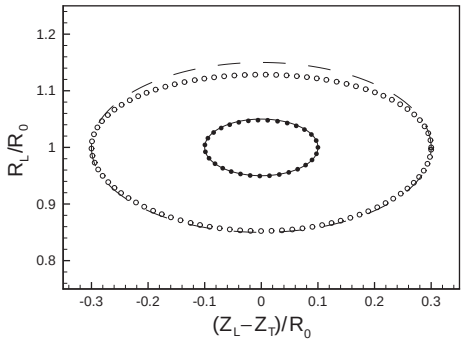

Fig. 3. Locus of the vortex cores calculated for two initial separations (solid line and filled symbols: $d/R_0 = 0.1$; dashed line and empty symbols: $d/R_0 = 0.3$), using the two-dimensional model (22) (lines) and the three-dimensional model (40) (symbols).

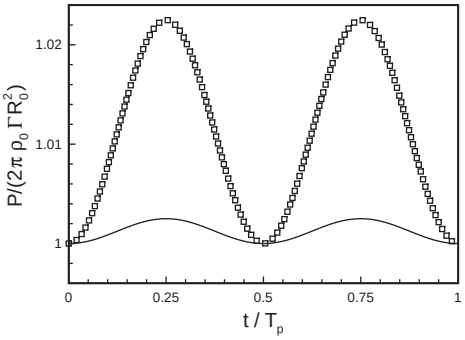

Fig. 4. Variations of impulse (8) of the system of two vortex rings following the two-dimensional model (22) for two initial separations (line: $d/R_0 = 0.1$; symbols: $d/R_0 = 0.3$).

be introduced in the next section (that takes into account vortex stretching). The difference becomes significant for $d/R_0 \geqslant 0.3$. One observes a flattening of the trajectory calculated using the more realistic three-dimensional model (Fig. 3). A consequence of the absence of variation in the self-induced velocity in the model is that the impulse and kinetic energy of the vortex system are not conserved. This is verified by substitution of Eq. (22) in definitions (8) and (10):

$$P = 2\pi\rho_0\Gamma R_0^2\left[1 + \frac{d^2}{4R_0^2}\sin^2\left(\frac{\Gamma t}{\pi d^2}\right)\right], \tag{24}$$

$$T = 2\pi\rho_0\Gamma\left[2R_0^2u_0 - \frac{\Gamma R_0}{2\pi} + \left(\frac{u_0d^2}{2} - \frac{\Gamma R_0}{2\pi}\right)\sin^2\left(\frac{\Gamma t}{\pi d^2}\right) - \frac{u_0\Gamma}{4\pi}\,t\sin\left(\frac{2\Gamma t}{\pi d^2}\right)\right]. \tag{25}$$

One sees that the impulse P contains a fluctuating component, scaling with d^2/R_0^2 and which is probably small in the asymptotic case $R_0 \gg d$ considered. This is illustrated in Fig. 4 for two values of the initial separation ($d/R_0 = 0.1$ and 0.3), where the impulse is normalized by the quantity $2\pi\rho_0\Gamma R_0^2$ to highlight the relative importance of the fluctuating component. Given the high acoustic efficiency of the dipolar radiation associated with a variation of impulse (see Eq. (7)), this small term alters the prediction of the radiated sound field.

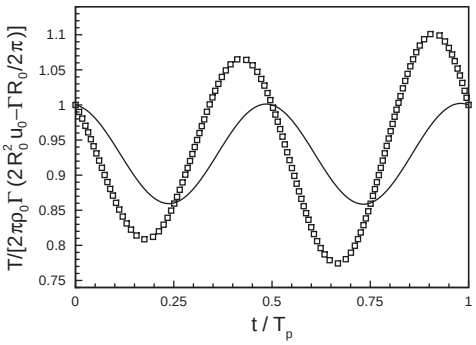

Fig. 5. Variations of the kinetic energy (10) of the system of two vortex rings following the two-dimensional model (22) for two initial separations (line: $d/R_0 = 0.1$; symbols: $d/R_0 = 0.3$).

The evolution of the kinetic energy T (normalized by $2\pi\rho_0\Gamma(2R_0^2u_0 - \Gamma R_0/2\pi)$, Fig. 5) confirms the shortcoming of the simplified model, in a more crucial way: in addition to an harmonically fluctuating component, one can observe an unrealistic term, with an amplitude increasing linearly with time. As time increases the model failure becomes more dramatic. This secular term could come from the singularity of the velocity field at the location of the filament that has not been taken into account in the calculation of the kinetic energy (25). A correct treatment of the singularity is provided by Lamb [15] and Saffman [14].

Substituting the vortex evolution (22) into Powell's formulation (19) gives

$$p'_P(\mathbf{x},t) = \frac{\rho_0}{4c_0^2|\mathbf{x}|^3}\left\{\left[\left(-\frac{4\Gamma^4R_0}{\pi^3d^4} + \frac{3\Gamma^3u_0}{\pi^2d^2}\right)\cos\left(\frac{2\Gamma t}{\pi^2d^2}\right) - \frac{2\Gamma^4u_0}{\pi^3d^4}\,t\sin\left(\frac{2\Gamma t}{\pi^2d^2}\right)\right]\mathbf{x}\cdot(\mathbf{nn})\cdot\mathbf{x} + \left(\frac{2\Gamma^4R_0}{\pi^3d^4} - \frac{\Gamma^3u_0}{\pi^2d^2}\right)\cos\left(\frac{2\Gamma t}{\pi^2d^2}\right)(\mathbf{x}\cdot\mathbf{x})\right\}, \tag{26}$$

in which the presence of a secular term invalidates the result. Applying the same algebra, Möhring's analogy (20) gives

$$p'_M(\mathbf{x},t) = \frac{\rho_0}{4c_0^2|\mathbf{x}|^3}\left[\left(\frac{3\Gamma^3u_0}{\pi^2d^2} - \frac{4\Gamma^4R_0}{\pi^3d^4}\right)\cos\left(\frac{2\Gamma t}{\pi^2d^2}\right) - \frac{2\Gamma^4u_0}{\pi^3d^4}\,t\sin\left(\frac{2\Gamma t}{\pi^2d^2}\right)\right]\mathbf{x}\cdot\left(\mathbf{nn} - \frac{\mathbf{I}}{3}\right)\cdot\mathbf{x}, \tag{27}$$

and once again a secular term appears.

Clearly, the direct application of both Powell and Möhring analogies in their original forms (respectively Eqs. (19) and (20)) to predict the sound radiated by the leapfrogging of two vortex rings as described by the planar flow model (22) is a failure.

These results show also that the singularity of the velocity field at the vortex filament corrupts the sound predicted by Möhring's analogy (20) even if the velocity does not appear explicitly in

the source term. The secular term in the sound predicted is related to the one that appears in the kinetic energy (25).

Möhring [2] found a way to compensate for such a weakness in the description of the flow by imposing one more time the conservation of the kinetic energy. This compensates the effect of the actual non-conservative character of the flow model. It will be shown below that the same derivation can be implemented into Powell's analogy, leading to the same formulation.

Using Lamb's results [15] and assuming that the total impulse of the flow is constant, one can express the first time derivative of Möhring's source integral (21) as a function of the kinetic energy:

$$\frac{\mathrm{d}Q}{\mathrm{d}t} = \frac{T}{2\pi\rho_0} + 3\int\int_{\boldsymbol{S}} \omega v r z \,\mathrm{d}r\,\mathrm{d}z. \tag{28}$$

The axial position of the vortex centroid can be defined as

$$z_0 = \frac{\int\int_{\boldsymbol{S}} \omega r^2 z \,\mathrm{d}r\,\mathrm{d}z}{\int\int_{\boldsymbol{S}} \omega r^2 \,\mathrm{d}r\,\mathrm{d}z} \tag{29}$$

and injecting the flow model (22) into this definition shows that $z_0 \simeq u_0 t$ in the asymptotic limit $d \ll R_0$ considered. Assuming the conservation of the impulse, one has

$$\int\int_{\boldsymbol{S}} \omega v r \,\mathrm{d}r\,\mathrm{d}z = 0, \tag{30}$$

so that Eq. (28) can be rewritten as

$$\frac{\mathrm{d}Q}{\mathrm{d}t} = \frac{T}{2\pi\rho_0} + 3\int\int_{\boldsymbol{S}} \omega v r\,(z - z_0)\,\mathrm{d}r\,\mathrm{d}z. \tag{31}$$

Although not explicitly specified by Möhring [2], this last expression is useful since it allows one to remove the presence of the mean convection velocity u_0 in the sound prediction (27). The sound production should theoretically not be affected by the value of the mean axial velocity of the vortex system. One finds

$$\frac{\mathrm{d}Q}{\mathrm{d}t} = \frac{T}{2\pi\rho_0} + \frac{3\Gamma^3 R_0}{4\pi}\left[1 + \cos\left(\frac{2\Gamma t}{\pi d^2}\right)\right], \tag{32}$$

and imposing the conservation of the kinetic energy, one finally obtains

$$\frac{\mathrm{d}^3 Q}{\mathrm{d}t^3} = -\frac{3\Gamma^4 R_0}{\pi^3 d^4}\cos\left(\frac{2\Gamma t}{\pi d^2}\right). \tag{33}$$

Möhring's result [2] is finally obtained by substitution of the last expression in Eq. (20):

$$p'_M(\mathbf{x}, t) = -\frac{3}{4}\frac{\rho_0 \Gamma^4 R_0}{\pi^3 d^4 c_0^2 |\mathbf{x}|^3}\cos\left(\frac{2\Gamma t}{\pi d^2}\right)\mathbf{x}\cdot\left(\mathbf{nn} - \frac{\mathbf{I}}{3}\right)\cdot\mathbf{x}. \tag{34}$$

The sound prediction (34) is compared in Fig. 6 to the prediction obtained by straightforward application of definition (20) using the three-dimensional leapfrogging model that will be presented in the next section, which respects the conservation of both the impulse and kinetic energy. It can be seen that in spite of the effective non-conservation of these quantities by the two-dimensional flow model, an accurate prediction is obtained.

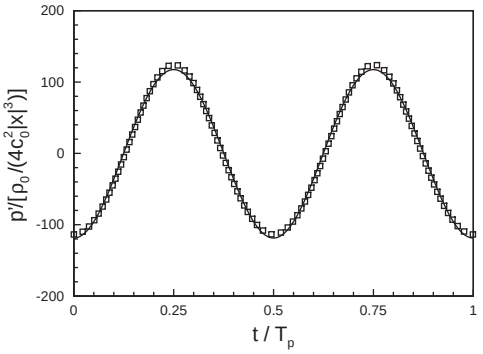

Fig. 6. Sound prediction obtained by the analytical expression (34) for the two-dimensional leapfrogging model (22) (line) compared to the prediction obtained using the three-dimensional model (40) (symbols); $d/R_0 = 0.1$. The listener's position $\mathbf{x}$ is set at a unit distance on the axis of symmetry and T_p is the period of the leapfrogging.

The same methodology can be followed within the framework of Powell's analogy, observing that

$$\frac{\mathrm{d}}{\mathrm{d}t}\left(\int\int_S \omega r^2 z \,\mathrm{d}r\,\mathrm{d}z\right) = 2\int\int_S \omega v r z \,\mathrm{d}r\,\mathrm{d}z + \int\int_S \omega u r^2 \,\mathrm{d}r\,\mathrm{d}z, \tag{35}$$

which is the bracketed expression in Eq. (19), then, equating the right side of Eqs. (28) and (35), gives

$$\int\int_S \omega u r^2 \,\mathrm{d}r\,\mathrm{d}z = \frac{T}{2\pi\rho_0} + \int\int_S \omega r v z \,\mathrm{d}r\,\mathrm{d}z, \tag{36}$$

so that the term to derive with respect to time in Eq. (19) can be written as

$$\begin{aligned}&\left(2\int\int_S \omega v r z \,\mathrm{d}r\,\mathrm{d}z + \int\int_S \omega u r^2 \,\mathrm{d}r\,\mathrm{d}z\right)\mathbf{x}\cdot(\mathbf{nn})\cdot\mathbf{x} - \left(\int\int_S \omega u r^2 \,\mathrm{d}r\,\mathrm{d}z\right)(\mathbf{x}\cdot\mathbf{x})\\ &\quad = \frac{T}{2\pi\rho_0}\mathbf{x}\cdot(\mathbf{nn}-\mathbf{I})\cdot\mathbf{x} + 3\left(\int\int_S \omega v r z \,\mathrm{d}r\,\mathrm{d}z\right)\mathbf{x}\cdot\left(\mathbf{nn}-\frac{\mathbf{I}}{3}\right)\cdot\mathbf{x}.\end{aligned} \tag{37}$$

Hence, subtracting the term $T/(2\pi\rho_0)\,\mathbf{x}\cdot(\mathbf{nn}-\mathbf{I})\cdot\mathbf{x}$ from Eq. (37), and subtracting the term $T/(2\pi\rho_0)$ from Eq. (28), both Powell's and Möhring's analogies (19) and (20) lead to the same expression

$$p'_{\mathrm{c}}(\mathbf{x},t) = \frac{3\rho_0}{4c_0^2|\mathbf{x}|^3}\frac{\mathrm{d}^2}{\mathrm{d}t^2}\left[\int\int_S \omega v r z \,\mathrm{d}r\,\mathrm{d}z\right]\mathbf{x}\cdot\left(\mathbf{nn}-\frac{\mathbf{I}}{3}\right)\cdot\mathbf{x}. \tag{38}$$

Finally, following the approach of Möhring, one can subtract the axial co-ordinate of the vortex centroid z_0 (29) to the co-ordinate of each element of vorticity (which is correct as far as the impulse is conserved), and obtain

$$p'_{\mathrm{c},0}(\mathbf{x},t) = \frac{3\rho_0}{4c_0^2|\mathbf{x}|^3}\frac{\mathrm{d}^2}{\mathrm{d}t^2}\left[\int\int_S \omega v r (z-z_0) \,\mathrm{d}r\,\mathrm{d}z\right]\mathbf{x}\cdot\left(\mathbf{nn}-\frac{\mathbf{I}}{3}\right)\cdot\mathbf{x}. \tag{39}$$

This is called the conservative formulation of the Powell–Möhring analogy.

It will now be shown how the original formulations of Powell (19), Möhring (20) and the conservative forms (38) and (39) behave when applied to a model of vortex leapfrogging that respects the flow invariants, but is perturbed by noise.

5.2. Three-dimensional modelling

In this more realistic vortex pairing model, the vortex core radius σ is still assumed to be small compared to the initial separation d between the vortices, i.e., the interaction of vortex filaments is again considered. The distance d is, however, no longer small compared to the initial radius R_0 of the vortex rings. Vortex stretching is therefore taken into account by varying the core radius σ to maintain the volume of each ring constant [14]. It is further assumed that there is a uniform distribution of the vorticity in the core of the filament. Distortion of the vortex core is neglected. This model has been successfully used by Kambe and Minota [18] to predict the sound produced by the leapfrogging of two vortex rings.

The Biot–Savart induction is integrated over the whole rings, and vortex stretching is taken into account in the evaluation of the self-induced velocity of each ring [18]:

$$\begin{cases} \dfrac{\mathrm{d}Z_i}{\mathrm{d}t} = \dfrac{1}{R_i}\dfrac{\partial \Psi}{\partial R_i} + \dfrac{\Gamma_i}{4\pi R_i}\left[\log\left(\dfrac{8R_i}{\sigma_i}\right) - \dfrac{1}{4}\right], \\ \dfrac{\mathrm{d}R_i}{\mathrm{d}t} = -\dfrac{1}{R_i}\dfrac{\partial \Psi}{\partial Z_i}, \\ \dfrac{\mathrm{d}\sigma_i^2 R_i}{\mathrm{d}t} = 0, \end{cases} \tag{40}$$

where the stream function associated with the vortex filament j, and evaluated at the vortex filament i is [15,19]:

$$\Psi = \frac{\Gamma_j}{2\pi}\sqrt{R_i R_j}\left[\left(\frac{2}{k_{ij}} - k_{ij}\right)\mathrm{K}(k_{ij}) - \frac{2}{k_{ij}}\mathrm{E}(k_{ij})\right], \tag{41}$$

with

$$k_{ij} = \sqrt{\frac{4R_i R_j}{(Z_i - Z_j)^2 + (R_i + R_j)^2}}, \tag{42}$$

where $\mathrm{K}(k)$ and $\mathrm{E}(k)$ are, respectively, the complete elliptic integrals of first and second kind. It is noteworthy that the system of equations (40) has two integrals of motion expressing the conservation of linear momentum and energy.

The solutions obtained using the two-dimensional model of vortex pairing (22) and the three-dimensional model (40) can be compared in Fig. 3, illustrating the locus of the vortex cores for two initial distances d between the rings. It can be seen that the trajectories of the vortex filaments are quite similar for $d/R_0 = 0.1$, while the two-dimensional model (22) gave an unrealistic path for $d/R_0 \geqslant 0.3$.

5.2.1. Influence of random perturbations on sound prediction

A major concern is the robustness of the sound prediction when the analogies are applied to a flow data contaminated by errors, inherent to a measurement technique or a numerical method.

The key idea of this section is to explore the sensitivity of the predicted sound field to perturbations added to the solution of the flow field obtained using the leapfrogging model (40). Since the conservation of the impulse and kinetic energy are respected by this model, it will be possible to evaluate the effect of the perturbations on these flow invariants. Then, on the basis of the previous discussions about the successive assumptions that are involved in the different formulations of vortex sound theory, their respective robustness will be evaluated and related to the flow invariants.

The random errors come from the measurement uncertainty and concern the vortex ring characteristics (co-ordinates of the cores, circulations). The parameters of the vortex rings have been defined on the basis of the particle image velocimetry measurements discussed in another paper [20]. Vortex pairing in a harmonically excited free jet is considered. It has been seen that the initial spacing between the vortices is half the initial diameter, and the initial core size is about one-tenth of the initial ring diameter. The circulation of each vortex is about $0.55U_0D$, where D is the diameter of the nozzle and U_0 the mean flow velocity at the nozzle exit. The trajectory of the vortices has been integrated over 100 points covering one cycle (Fig. 7). As it can be verified from Figs. 8 and 9, the momentum conservation is accurately respected but fluctuations of 1% in the kinetic energy are observed. Hence without the use of the analogy of Powell or Möhring (Fig. 10) this model could not provide a correct prediction of the sound production by leapfrogging.

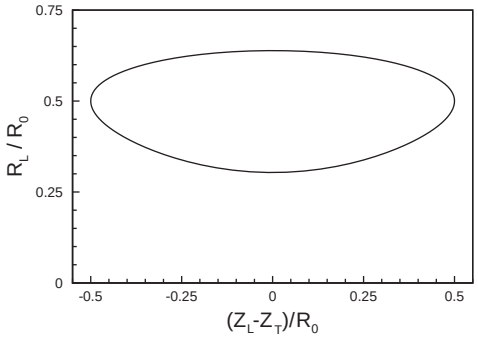

Fig. 7. Locus of the vortex rings calculated the three-dimensional model (40) for an initial axial separation $d/R_0 = 1$.

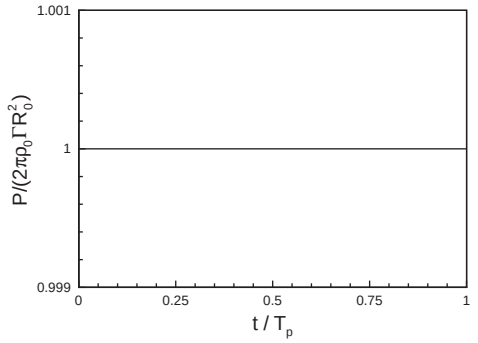

Fig. 8. Impulse P of the system of two vortex rings following the three-dimensional model (40) for an initial separation $d/R_0 = 1$.

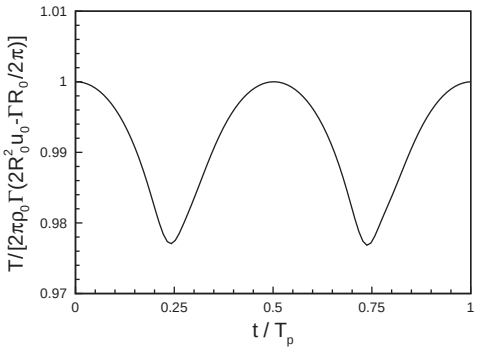

Fig. 9. Kinetic energy T of the system of two vortex rings following the three-dimensional model (40) for an initial separation $d/R_0 = 1$.

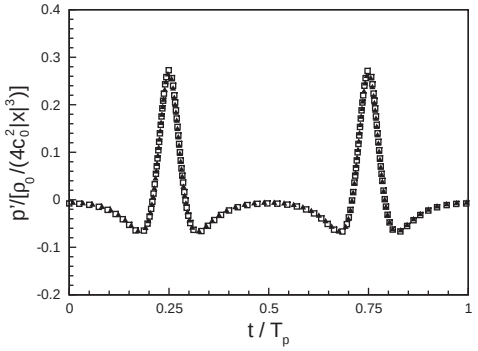

Fig. 10. Sound pressure level predicted by Möhring's (20) (▲) and Powell's (19) (□) original formulations applied to the unperturbed vortex ring evolutions (initial axial separation $d/R_0 = 1$).

Random (Gaussian) noise has been added to the vortex ring core co-ordinates as a first step, and to their circulation as a second step. The absolute root-mean square amplitudes of the noise added to the co-ordinates and circulations are, respectively, 10^{-5} and 10^{-4}, and the corresponding relative amplitudes are 0.002% and 0.02%. Please note that the perturbations have been added independently to each of the axial and radial co-ordinates of each vortex and to their individual circulations .

In what follows, the sensitivity of a quantity X to the addition of noise will be evaluated through the difference δX between its values for the perturbed and the unperturbed cases:

$$\delta X = X_{perturbed} - X_{unperturbed}. \tag{43}$$

The effect of the added noise on the flow invariants is indicated in Figs. 11–14. It is difficult to formulate conclusions from comparison of these figures, since the amplitudes of the perturbations of the co-ordinates and kinetic energy are not identical. Nevertheless, it appears clearly that perturbing the co-ordinates influences mostly the kinetic energy and leaves the impulse relatively unaffected. Adding noise to the circulation has the inverse effect.

The effect of the added noise is significant when considering the sound prediction (Figs. 15 and 16). It can be seen from Fig. 15 that applying the direct formulations of Powell and Möhring to

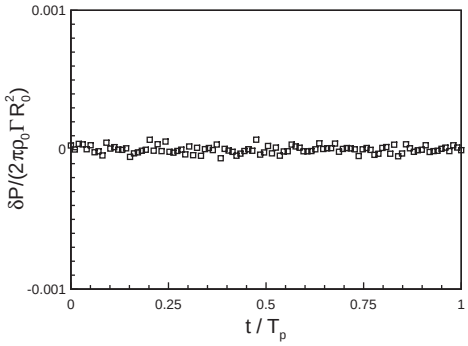

Fig. 11. Effect of 10^{-5} co-ordinate perturbation on impulse (8) (initial axial separation $d/R_0 = 1$).

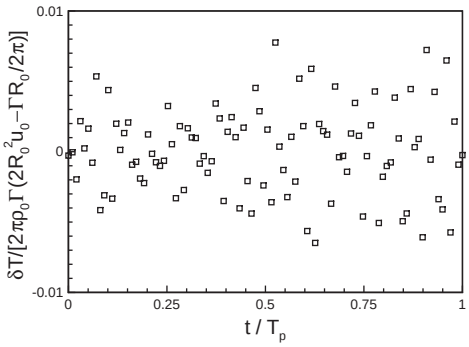

Fig. 12. Effect of 10^{-5} co-ordinate perturbation on kinetic energy (10) (initial axial separation $d/R_0 = 1$).

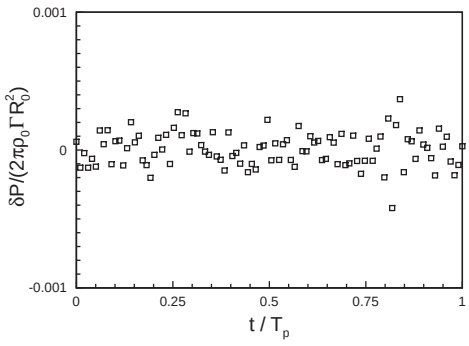

Fig. 13. Effect of 10^{-4} circulation perturbation on impulse (8) (initial axial separation $d/R_0 = 1$).

the perturbed co-ordinates case, the variation of the sound pressure $\delta p'$ exhibits a scatter as large as the sound pressure p' itself.

Fig. 16 shows that Powell's analogy performs much better when one considers the perturbed circulation case. The additional time derivative required in Möhring's formulation explains this result.

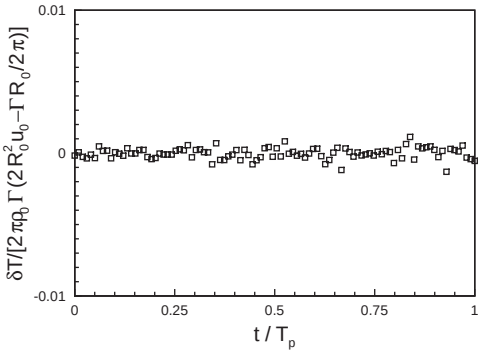

Fig. 14. Effect of 10^{-4} circulation perturbation on kinetic energy (10) (initial axial separation $d/R_0 = 1$).

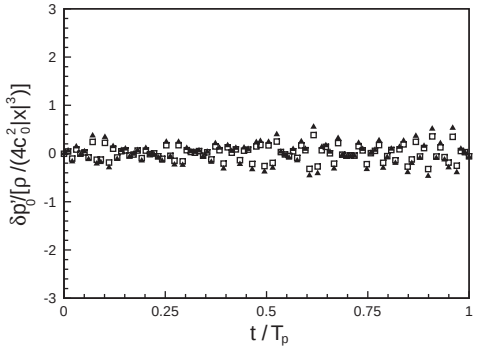

Fig. 15. Error on sound predicted by Möhring's (20) (□) and Powell's (19) (▲) original formulations applied to the 10^{-5} perturbed vortex ring co-ordinates.

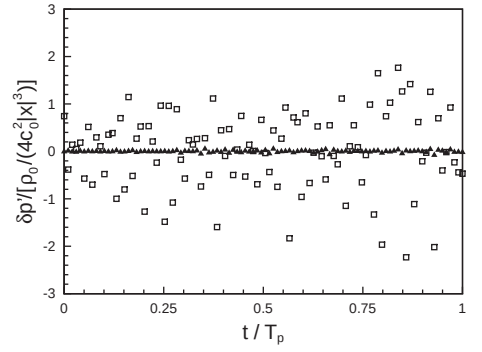

Fig. 16. Error on sound predicted by Möhring's (20) (□) and Powell's (19) (▲) original formulations applied to the 10^{-4} perturbed vortex ring circulations.

A somewhat surprising result is that Möhring's formulation (20) produces slightly less scatter than Powell's equation (19) when perturbation of the co-ordinates is considered, in spite of its additional time derivative. This robustness might be a consequence of the additional assumption of conservation of the kinetic energy that is incorporated in Möhring's analogy. In the case of the

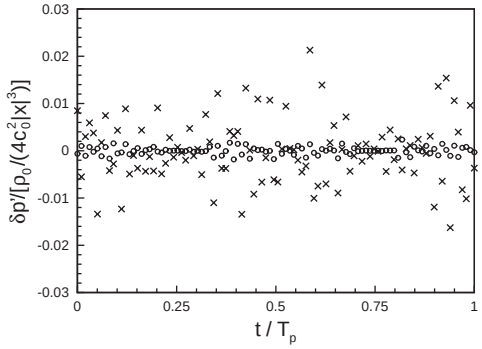

Fig. 17. Error on sound predicted by the conservative formulation (39) applied to the vortex ring evolutions perturbed on either trajectories (noise amplitude 10^{-5}, $\times$ symbols) or circulations (noise amplitude 10^{-4}, $\circ$ symbols), initial axial separation $d/R_0 = 1$.

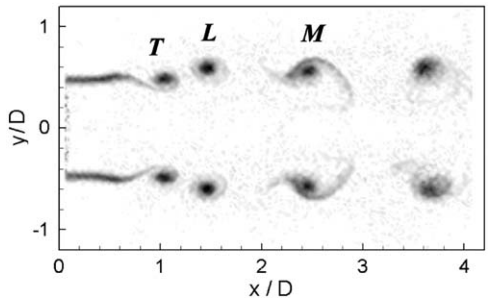

Fig. 18. Sample vorticity field obtained using particle image velocimetry in an acoustically excited subsonic free jet.

two-dimensional model of leapfrogging (Section 5.1) the circulation was conserved but an error was introduced in the co-ordinates. It was also observed in that case that Möhring's approach performed well.

Finally, Fig. 17 shows that the scatter of $\delta p'$ calculated using the conservative formulation (39) is about 20 times smaller that what was obtained using Powell's analogy for the perturbed circulation case. The scatter is larger for the perturbed co-ordinates case, but remains still about 30 times smaller that using Möhring's and Powell's analogies. This success is due to the fact that an additional time momentum and energy conservation by using Lamb's [15] equation (31) has been imposed.

5.3. Experimental description of vortex pairing measured by PIV

Finally, the different forms of the acoustical source term (21), (28) and (31) have been calculated from experimental data obtained in an acoustically excited subsonic jet using the particle image velocimetry (PIV) measurement technique. The jet outlet velocity is $U_0 = 5$ m/s and the nozzle outlet diameter $D = 0.041$ m. The details of the experimental arrangement and of the procedure used to process the data are indicated in another paper [20]. A typical

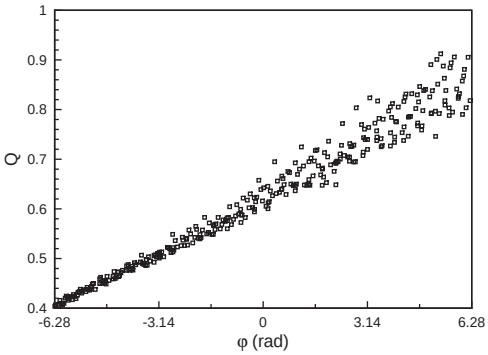

Fig. 19. Acoustical source term Q (21) obtained from the experimental data.

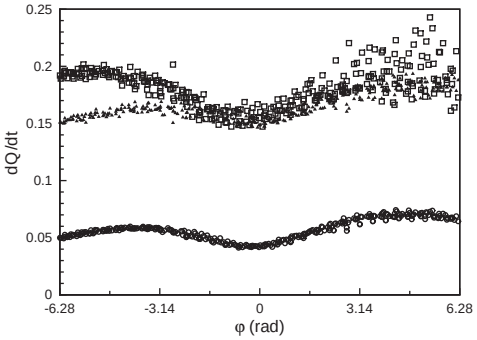

Fig. 20. Acoustical source term $\mathrm{d}Q/\mathrm{d}t$ obtained from the experimental data. □, formulation (28); ▲, formulation (31); ◦, formulation (31) $-T/2\pi\rho_0$.

vorticity field obtained from the PIV measurements is shown in Fig. 18, where the leading and trailing vortices are, respectively, designated by L and T and the merged ring is indicated by M. We use series of 32 of such measurements distributed over two excitation periods, obtained by means of a stroboscopic method [21]. Fig. 19 shows the acoustical source term (21) that has been calculated on the basis of the experimental data. It can be anticipated that the calculation of the subsequent three time derivatives that are required in Eq. (20) will be spoiled by the measurement noise. The first derivative of the acoustic source term (28) that is shown in Fig. 20 presents also some scatter, but its order of magnitude is much smaller. When using formulation (31), the scatter is even more reduced. Finally, when the kinetic energy term $T/2\pi\rho_0$ is subtracted from Eq. (31) anticipating the time derivation in Eq. (39), the scatter is again reduced. This demonstrates the effectiveness of formulation (39) regarding the robustness of the prediction using a description of the flow that is noisy and/or does not respect exactly the conservation of momentum and kinetic energy. The successive corrections that have been brought seem to compensate for the inaccuracies that are inherent to the experimental description of the flow field.

6. Conclusions

An explicit description of the steps used to obtain a useful prediction of the aero-acoustic sound field from simplified models of the flow at low Mach numbers has been provided. It has been argued that the analogies of Lighthill [4,6], Powell [9] and Möhring [2] provide explicit expressions for the contributions of various physical phenomena to sound radiation. This allows the correction of the prediction by imposing conservation of momentum or energy even when the flow model does not respect these fundamentals laws.

Lighthill's analogy provides a prediction of a quadrupole radiation in free turbulence by suppressing the monopole and dipole terms, which corresponds to the reinforcement of the laws of mass and momentum conservation. Powell's vortex sound theory (11) starts from Lighthill's approach followed by an additional use of the laws of momentum and energy conservation. Möhring's vortex sound analogy (16) is derived from Powell's formulation using Helmholtz's equation and assuming once more the conservation of energy.

When the original approaches of Powell and Möhring are applied to a two-dimensional model for ring vortex pairing, an unrealistic solution is obtained. This failure is related to the non-conservation of the momentum and kinetic energy (and in particular to the secular evolution of the latter). Nevertheless, a reasonable prediction of the sound production is obtained when the assumptions of conservation of these invariants are reiterated in the derivation of (32).

Following this concept due to Möhring [2], two conservative formulations (38) and (39) have been derived for axisymmetrical flows by reiterating the hypotheses of conservation of momentum and energy.

The sensitivity of the vortex sound analogy to noise perturbing the flow model has been investigated. A three-dimensional (axisymmetric) flow model that takes into account vortex stretching but no core distortion provides the reference flow evolution in which the momentum and energy are conserved. The approach of Möhring has the drawback to involve a third time derivative, while Powell only needs a second time derivative. Results show that Powell's original formulation (19) provides indeed better results when the ring circulation is perturbed (which affects mostly the conservation of impulse). However, Möhring's formulation (20) performs slightly better than Powell's formulation (19) when the ring co-ordinates are perturbed (which has the larger effect on the kinetic energy conservation). The additional energy conservation assumption that is incorporated into Möhring's analogy explains this result.

The application of the conservative form (39) to the perturbed flow cases reduces the scatter in the sound prediction. In the analysis of the vortex pairing model this scatter is about 20–30 times smaller compared to the scatter in the results of the original formulations of Möhring and Powell.

Finally, the different formulations have been compared using experimental PIV data of vortex pairing in a subsonic free jet. The results confirm the better performance of formulation (31), in particular when kinetic energy conservation is reinforced an additional time.

References

[1] A.T.F. Fedorchenko, On some fundamental flaws in present aeroacoustic theory, Journal of Sound and Vibration 232 (4) (2000) 719–782.

[2] W. Möhring, On vortex sound at low Mach number, Journal of Fluid Mechanics 85 (1978) 685–691.

[3] D.G. Crighton, A.P. Dowling, J.E.F. Williams, M. Heckl, F.G. Leppington, Modern Methods in Analytical Acoustics—Lecture Notes, Springer, Berlin, 1992.
[4] M.J. Lighthill, On sound generated aerodynamically. Part I. General theory, Proceedings of the Royal Society, London A 211 (1952) 564–587.
[5] C.K.W. Tam, On the failure of the acoustic analogy theory to identify the correct noise sources, Proceedings of the Seventh AIAA/CEAS Aeroacoustics Conference, Maastricht, The Netherlands, 2001, pp. 2001–2117.
[6] M.J. Lighthill, On sound generated aerodynamically. Part II. Turbulence as a source of sound, Proceedings of the Royal Society, London A 222 (1954) 1–32.
[7] C.L. Morfey, Sound radiation due to unsteady dissipation in turbulent flows, Journal of Sound and Vibration 48 (1984) 95–111.
[8] F. Obermeier, Aerodynamic sound generation caused by viscous processes, Journal of Sound and Vibration 99 (1985) 111–120.
[9] A. Powell, Theory of vortex sound, Journal of the Acoustical Society of America 36 (1) (1964) 177–195.
[10] T. Kambe, T. Minota, Acoustic emissions by vortex motions, Journal of Fluid Mechanics 173 (1986) 643–666.
[11] M.S. Howe, The dissipation of sound at an edge, Journal of Sound and Vibration 70 (1980) 407–411.
[12] A. Hirschberg, C. Schram, in: Y. Aurégan, A. Maurel, V. Pagneux, J.-F. Pinton (Eds.), A Primitive Approach in Aeroacoustics, Lecture Notes in Physics, Vol. 586, Springer, Berlin, 2002, pp. 1–30.
[13] B.K. Batchelor, An Introduction to Fluid Dynamics, Cambridge University Press, Cambridge, 1967.
[14] P.G. Saffman, Vortex Dynamics, Cambridge University Press, Cambridge, 1992.
[15] H. Lamb, Hydrodynamics, Cambridge University Press, Cambridge, 1932.
[16] A. Powell, Vortex sound theory: direct proof of equivalence of "vortex force" and "vorticity-alone" formulations, Journal of the Acoustical Society of America 97 (1995) 1534–1537.
[17] A. Powell, Vortex sound: an alternative derivation of Möhring's formulation, Journal of the Acoustical Society of America 97 (1995) 684–686.
[18] T. Kambe, T. Minota, Sound radiation from vortex systems, Journal of Sound and Vibration 74 (1) (1981) 61–72.
[19] F.W. Dyson, The potential of an anchor ring. Part II, Philosophic Transactions of the Royal Society, London A 184 (1983) 1041–1106.
[20] C. Schram, A. Hirschberg, R. Verzicco, Sound produced by vortex pairing: prediction based on particle image velocimetry, Proceedings of the Eighth AIAA/CEAS Aeroacoustics Conference, Breckenridge, Colorado, 2002, pp. 2002–2526.
[21] C. Schram, M.L. Riethmuller, Measurement of vortex ring characteristics during pairing in a forced subsonic air jet, Experiments in Fluids 33 (2002) 879–888.